Journal of Alloys and Compounds 615 (2014) S98–S101

Contents lists available at ScienceDirect

Journal of Alloys and Compounds

journal homepage: www.elsevier.com/locate/jalcom

Indentation size effect in metallic glasses: Mean pressure at the initiation of plastic flow ☆

S. Nachum [a,*], A.L. Greer [a,b]

[a] Department of Materials Science & Metallurgy, University of Cambridge, 27 Charles Babbage Road, Cambridge CB3 0FS, United Kingdom
[b] WPI-Advanced Institute for Materials Research (WPI-AIMR), Tohoku University, Sendai 980-8577, Japan

ARTICLE INFO

Article history:
Available online 15 December 2013

Keywords:
Metallic glasses
Mechanical properties
Nanoindentation
Plastic yielding
Shear band

ABSTRACT

Nanoindentation tests using a spherical indenter of tip radius 10 μm have been performed on Zr- and Pd-based metallic glasses, focusing on the cumulative distribution of the first yield load. When normalized using the macroscopic yield stress, the distribution of mean pressure at yield is nearly independent of the glass composition. Collecting literature data, there is a clear indentation size effect in metallic glasses: the smaller the indenter tip radius, the larger the indentation pressure at yield. The magnitude of the size effect in metallic glasses is compared with, and found to lie between, the cases of crystalline metals and ceramics.

1. Introduction

Nanoindentation is widely used for measuring mechanical properties, with the advantages of small probe volume and a short test time; >100 tests can be completed in a few hours. Using a spherical indenter tip means that stresses and strains increase gradually as the tip penetrates further into the material, and plastic flow is delayed to greater penetration depths; this facilitates measurement of the elastic properties of the indented material.

In comparison to polycrystalline metals, metallic glasses (MGs) show higher yield strength but minimal ductility [1], and their macroscopic yield strain is approximately constant at 2% [2]. Similar to polycrystalline metals, yield in MGs is due to a maximum shear stress and is only slightly sensitive to hydrostatic pressure [3]. Under quasi-static loading and well below the glass-transition temperature, plastic flow of metallic glasses is by shear-banding (e.g. [4–6]). In nanoindentation under load-control, the onset of plastic flow, involving nucleation and propagation of shear bands, is detected on the load–penetration curve as a sudden penetration burst at a constant load. With a spherical tip the first "pop-in" event is easily detected on the loading curve.

The initial yield load of MGs, determined from such pop-ins, has been studied extensively [7–13], and can vary from one point to point in the bulk material. Packard et al. [13] showed that the distribution in the first yield load is due to variations in the sampled structure of the MG and, in contrast to crystalline metals, is not very sensitive to loading rate or temperature. The width of the distribution increases as the stressed volume decreases. The indentation pressure at the first yield load is much higher than the macroscopic yield pressure given by the classical Hertzian solution. Packard and Schuh [7] postulated that the yield pressure is so high because the stress along the entire path of a potential shear band, from the nucleation point underneath the tip up to the free surface, must exceed the macroscopic yield strength of the MG, before the band can operate. However, recent results [9,14] suggest that the high pressure at yield is due to the small potential plastic zone, the yield pressure and tip radius having a power-law relationship with an exponent of −0.2.

2. Experimental procedures

Two Pd-based and two Zr-based MGs, $Pd_{40}Cu_{30}Ni_{10}P_{20}$, $Pd_{77.5}Cu_6Si_{16.5}$, $Zr_{60}Cu_{20}Fe_{10}Al_{10}$ and $Zr_{57}Ti_5Cu_{20}Ni_8Al_{10}$ (at.%) were prepared by arc melting the pure elements under Ar atmosphere, followed by casting into a copper mould using standard procedures (e.g. as in Refs. [15,16]). The first three compositions were cast as rods of diameter 5, 2 and 6 mm respectively; the fourth was cast as a plate $15 \times 10 \times 2.5$ mm^3. Their amorphicity was confirmed by X-ray diffraction. Discs 2 mm thick were cut from the as-cast rods for the indentation tests. The samples were cold-mounted in a resin and mechanically polished to a mirror finish, finally with 60 nm colloidal silica particles.

Nanoindentation (MTS Nanoindenter XP) was performed under load control using a diamond spherical indenter of tip radius 10.37 μm. In all tests the loading and unloading rates were 0.5 mN s^{-1} and the thermal drift was kept below 8×10^{-2} nm s^{-1}. The area function of the indenter tip and the machine compliance were calibrated using indentation of a fused-silica standard.

The Vickers hardness H_0 of the glasses was measured at a 20 N load, and had average values of 4.6 GPa ($Pd_{40}Cu_{30}Ni_{10}P_{20}$), 4.3 GPa ($Pd_{77.5}Cu_6Si_{16.5}$), 4.7 GPa ($Zr_{60}Cu_{20}Fe_{10}Al_{10}$) and 4.8 GPa ($Zr_{57}Ti_5Cu_{20}Ni_8Al_{10}$). The compressive yield strength σ_y is taken to be $H_0/3$.

* Corresponding author. Tel.: +44 1223334300.
E-mail address: sn341@cam.ac.uk (S. Nachum).

0925-8388/$ - see front matter © 2014 The Authors. Published by Elsevier B.V. All rights reserved.
http://dx.doi.org/10.1016/j.jallcom.2013.12.058

The Hertzian elastic solution for normal indentation of an elastic–ideal plastic half-space by a frictionless sphere of radius R is [17]:

$$F = (4/3)E_r(a^3/R), \quad (1)$$

where F is the applied load, a is the contact radius, and E_r is the indentation modulus related to the elastic moduli (E_g, E_i) and the Poisson ratios (ν_g, ν_i) of the glass and of the indenter through:

$$1/E_r = \left(1 - \nu_g^2\right)/E_g + (1 - \nu_i^2)/E_i. \quad (2)$$

The mean pressure underneath the indenter, P, is given by the load F normalized by the indentation contact area:

$$P = F/\pi a^2 = (4/3\pi)(a/R)E_r. \quad (3)$$

In the elastic regime, a is related to the total indentation displacement h according to:

$$a = \sqrt{Rh}, \quad (4)$$

provided that h is small compared to R.

We focus on how R affects the initial yield pressure (P_y) of the glass. P_y is revealed from the $F - h$ curve by the first sudden displacement burst that occurs at a yield displacement h_y and at a yield load F_y, marking the transition between Hertzian elastic contact and subsequent elastic–plastic contact:

$$P_y = F_y/\pi a_y^2 = F_y/(\pi R h_y). \quad (5)$$

Yielding of MGs is initiated at the location of maximum shear stress τ_{max} in the stressed volume [1]. In spherical indentation of an elastic–ideal plastic solid, τ_{max} is located ~0.5a below the surface, along the axis of contact [17]. For Zr-based glasses with typical Poisson ratio $\nu = 0.37$, $\tau_{max} \approx 0.44P_y$; for Pd-based glasses ($\nu = 0.41$), $\tau_{max} \approx 0.43P_y$, a negligible difference [17,18]. Using the Tresca yield criterion, where $\tau_y = \sigma_y/2$ [17], P_y is proportional to yield stress σ_y:

$$P_y = 1.1\sigma_y. \quad (6)$$

Using Eq. (3), the indentation strain at initial yield is proportional to the yield strain:

$$(a_y/R) \approx 2.6\ (\sigma_y/E_r). \quad (7)$$

3. Results and discussion

3.1. Cumulative distribution of yield load and yield pressure

Fig. 1(a) shows the cumulative distribution of the first yield load F_y for >100 indents for each glass. Each glass has a characteristic distribution and median value of F_y. The same data can be plotted against the normalized yield pressure P_y/σ_y (Fig. 1(b)), in which case all four distributions fall approximately onto a single curve. For the glasses tested here, the median value of P_y/σ_y is nearly independent of composition.

The median value of the normalized yield pressure is about three times the corresponding value for a macroscopic spherical indentation predicted from the Hertzian solution as given in Eqs. (6) and (7). Recalling that R = 10.37 μm, the high value of P_y is attributed to the small deformed volume, limited by the small tip radius.

Fig. 1(b) suggests that the median value of P_y is approximately three times σ_y. We now show that P_y can be even higher if R is smaller than 10 μm.

3.2. Indentation size effect in metallic glasses

Data on F_y for a range of metallic glasses [8–12], all indented with a spherical tip (180 nm < R < 31.5 μm) are collected in Fig. 2. Each data point represents an average of ~100 indents. There is a clear indentation size effect: smaller R gives higher P_y/σ_y, according to a power law with exponent −0.18. Yield onset in MGs under a nanoindenter tip is presumed to be by the nucleation and propagation of a shear band when the stress acting is high enough to activate a critical cascade of shear transformation zones (STZs). But the probed volume can be so small that the low population of STZs inhibits shear-band nucleation. When the indentation length scale is large enough, P_y is simply the macroscopic yield strength of the glass (Eq. (6)); in this regime, plastic flow is controlled by the propagation of already nucleated shear bands originating from a collection of STZs with low activation barriers, or from processing flaws such as cracks or porosity [19]. When the indentation length scale is smaller, the population of easily activated STZs and flaws in the stressed volume becomes low and P_y increases, flow being controlled by heterogeneous nucleation of a shear band rather than propagation.

Fig. 2 suggests that this regime begins at $R \approx 1$ mm. In the limiting case, P_y approaches the theoretical strength of the glass. We predict that this upper limit for the pressure is ~8σ_y, as follows. The macroscopic yield strain of MGs is ~0.018, independent of composition [2]. The ratio of shear modulus G to Young's modulus E is ~3/8 for polycrystalline metals, ceramics and metallic glasses (e.g. [18]), suggesting that the macroscopic σ_y of MGs is ~G/20. Taking the theoretical strength of metallic glasses to be ~2G/5 [2], which is P_y for a perfect glass without structural defects, we find that $P_y/\sigma_y \approx 8$, a value reached at $R \approx 10$ nm (Fig. 2).

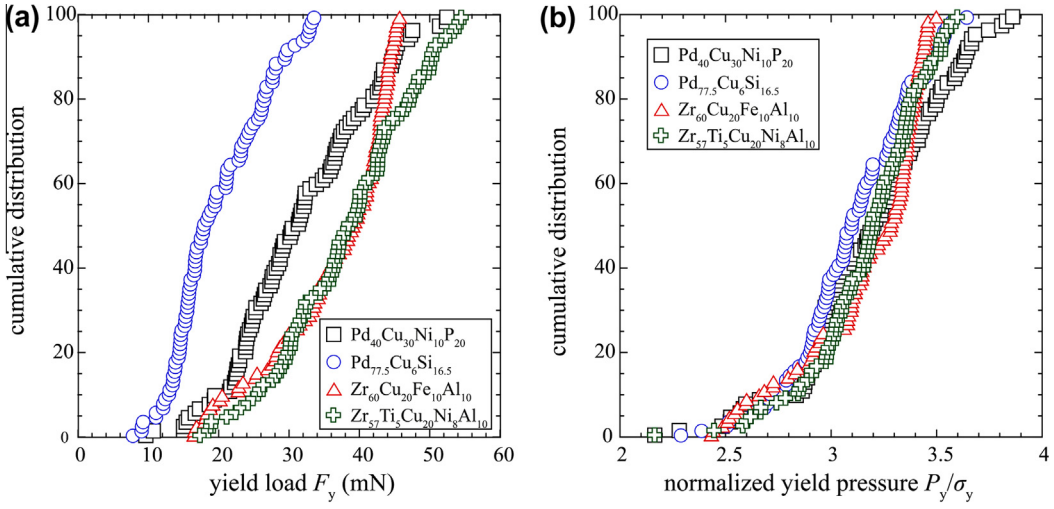

Fig. 1. Cumulative distribution of (a) the first yield load F_y and (b) the normalized yield pressure P_y/σ_y. All four distributions fall approximately on the same master curve when the yield pressure P_y is normalized by the macroscopic yield stress of the glass σ_y.

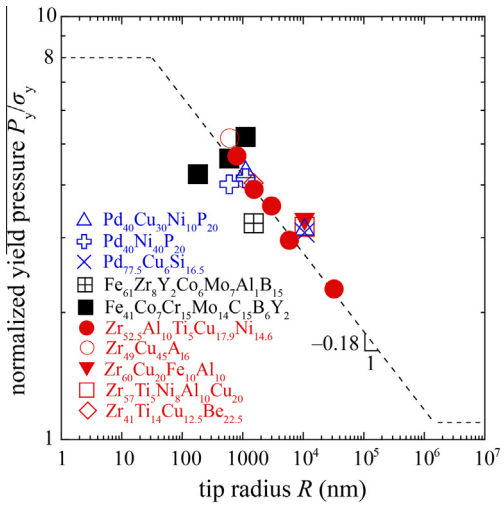

Fig. 2. Data from the literature [8–12] and from the present study of Zr, Pd-based metallic glasses plotted as the normalized yield pressure P_y/σ_y vs. indenter tip radius R.

Similar regimes controlled by shear-band propagation or nucleation are observed in micro-pillar compression of MGs (e.g. [19]). Even for the smallest diameter pillar, however, the measurements give $P_y/\sigma_y \approx 2$ [19]. The increase P_y in nanoindentation is because of the smaller potential plastic zone.

3.3. Comparison of metallic glasses, metals and ceramics

We now compare the indentation size effect in MGs with that in crystalline metals and ceramics. Zhu et al. [20] showed in nanoindentation using a spherical indenter tip that $P_y/P_0 \propto R^{-1/3}$. P_0 is a yield pressure obtained for each material when a linear fit to the P_y vs. $R^{-1/3}$ data is extrapolated to the ordinate, and the intercept corresponding to P_0. The indentation size effect is about 7 times greater for metals than for ceramics. Fig. 3 shows these data, together with the data for $Zr_{52.5}Cu_{17.9}Ni_{14.6}Al_{10}Ti_5$ MGs plotted in Fig. 2. For MGs, $P_y/P_0 \propto R^{-1/3}$ with a gradient smaller than for metals, but approximately 1.5 times that for ceramics. The same authors have shown [21,22] that P_y/P_0 of different ceramics and of tungsten is proportional to the inverse square root of the contact radius. Plotting P_y/P_0 against $a^{-1/2}$, the data for MGs are more scattered, only loosely fitting the linear relation, but still bounded between the data for ceramics and the data for tungsten. As noted by Zhu et al. [21], the plot P_y/P_0 vs. $a^{-1/2}$ introduces random errors in both ordinate and abscissa.

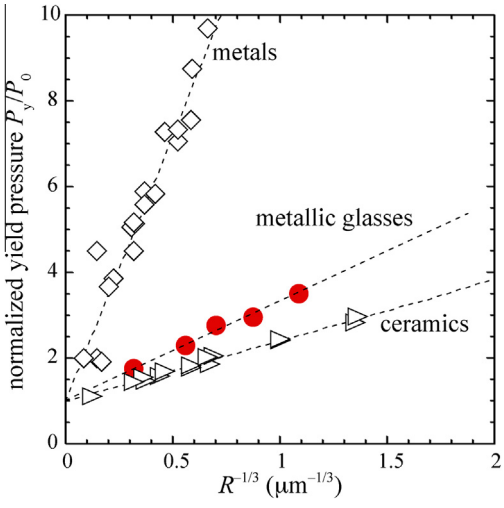

Fig. 3. Normalized yield pressure as a function of the inverse cube root of the tip radius, for metallic glasses, metals and ceramics. Data on metallic glasses as in Fig. 2; other data from Ref. [20].

Theories for the scaling with $R^{-1/3}$ and with $a^{-1/2}$ have been proposed. Gerberich et al. [23] reported that the hardness, rather than P_y, of a wide range of metals scales with $R^{-1/3}$ and explained the size effect in terms of the surface-to-volume ratio of the plastic zone. Bushby et al. [22] showed that the concept of dislocation slip distance generates a scaling with $a^{-1/2}$ and suggested that the magnitude of the indentation size effect is dictated by the square root of the ratio of yield strain to the magnitude of the Burgers vector. Whether the size effect in MGs scales better with the geometry of loading ($R^{-1/3}$) or with the geometry of contact ($a^{-1/2}$) is still not clear and remains open for future work. Nonetheless, Fig. 3 suggests, similar to conclusions drawn from the micropillar compression of crystalline solids, that the size effect is larger for softer solids [24]. We postulate that the magnitude of the indentation size effect scales inversely with the yield strain of the solid. Typical values of the yield strain for polycrystalline metals, metallic glasses and ceramics are 10^{-4}–10^{-3}, 2×10^{-2} and 10^{-2}–10^{-1}, respectively [25].

4. Conclusions

Four metallic glasses have been studied using nanoindentation with a spherical indenter tip. For the 10 μm tip radius used, the normalized yield pressure and the normalized indentation yield strain at the elastic limit are ~3 times those in the macroscopic regime (Hertzian solution). The increases in yield pressure and strain are independent of glass composition. Data collected for several metallic glasses suggest that the limiting value of the yield pressure is reached when the tip radius decreases to ~10 nm, when the potential plastic zone contains a low population of structural defects. The yield pressure for a defect-free glass is predicted to be about eight times its macroscopic yield strength. The indentation size effect in metallic glasses is bounded by the behaviour of crystalline ceramics and metals. We postulate that the magnitude of the indentation size effect in these solids is inversely correlated with their yield strain.

Acknowledgements

The research is funded by the Engineering and Physical Sciences Research Council, UK (Materials World Network project) and by the WPI-AIMR, Tohoku University. The authors thank T.C. Hufnagel (Johns Hopkins University) and Prof. Inoue (Tohoku University) for supplying the metallic-glass samples.

References

[1] C.A. Schuh, T.C. Hufnagel, U. Ramamurty, Acta Mater. 55 (2007) 4067–4109.
[2] W.L. Johnson, K. Samwer, Phys. Rev. Lett. 95 (2005) 195501.
[3] M.N.M. Patnaik, R. Narasimhan, U. Ramamurty, Acta Mater. 52 (2004) 3335–3345.
[4] C.A. Schuh, A.S. Argon, T.G. Nieh, J. Wadsworth, Philos. Mag. 83 (2003) 2585–2597.
[5] C.A. Schuh, A.C. Lund, T.G. Nieh, Acta Mater. 52 (2004) 5879–5881.
[6] A.L. Greer, Y.Q. Cheng, E. Ma, Mater. Sci. Eng., R 74 (2013) 71–132.
[7] C.E. Packard, C.A. Schuh, Acta Mater. 55 (2007) 5348–5358.
[8] C.E. Packard, E.R. Homer, N. Al-Aqeeli, C.A. Schuh, Philos. Mag. 90 (2010) 1373–1390.
[9] I.C. Choi, Y. Zhao, Y.J. Kim, B.G. Yoo, J.Y. Suh, U. Ramamurty, J.I. Jang, Acta Mater. 60 (2012) 6862–6868.
[10] N. Al-Aqeeli, J. Alloys Comp. 509 (2011) 7216–7220.
[11] L. Wang, H. Bei, Y.F. Gao, Z.P. Lu, T.G. Nieh, Acta Mater. 59 (2011) 7627–7633.
[12] H. Bei, Z.P. Lu, E.P. George, Phys. Rev. Lett. 93 (2004) 125504.
[13] C.E. Packard, O. Franke, E.R. Homer, C.A. Schuh, J. Mater. Res. 25 (2010) 2251–2263.

[14] I.C. Choi, Y. Zhao, B.G. Yoo, Y.J. Kim, J.Y. Suh, U. Ramamurty, J.I. Jang, Scr. Mater. 66 (2012) 923–926.
[15] L.Q. Xing, Y. Li, K.T. Ramesh, J. Li, T.C. Hufnagel, Phys. Rev. B 64 (2001) 180201.
[16] A. Inoue, N. Nishiyama, T. Matsuda, Mater. Trans. JIM 37 (1996) 181–184.
[17] K.L. Johnson, Contact Mechanics, Cambridge University Press, Cambridge, 1985.
[18] W.H. Wang, Prog. Mater. Sci. 57 (2012) 487–656.
[19] C.C. Wang, J. Ding, Y.Q. Cheng, J.C. Wan, L. Tian, Z.W. Shan, J. Li, E. Ma, Acta Mater. 60 (2012) 5370–5379.
[20] T.T. Zhu, X.D. Hou, A.J. Bushby, D.J. Dunstan, J. Phys. D: Appl. Phys. 41 (2008) 074004.
[21] T.T. Zhu, A.J. Bushby, D.J. Dunstan, J. Mech. Phys. Solids 56 (2008) 1170–1185.
[22] A.J. Bushby, T.T. Zhu, D.J. Dunstan, J. Mater. Res. 24 (2009) 966–972.
[23] W.W. Gerberich, N.I. Tymiak, J.C. Grunlan, M.F. Horstemeyer, M.I. Baskes, J. Appl. Mech. 69 (2002) 433–442.
[24] S. Korte, W.J. Clegg, Philos. Mag. 91 (2011) 1150–1162.
[25] M.F. Ashby, Materials Selection in Mechanical Design, second ed., Butterworth-Heinemann, Oxford, 1999.